Mondragon Unibertsitatea Biblioteka Biblioteca

biblioteka@mondragon.edu

This is an Accepted Manuscript version of the following article, accepted for publication in:

U. Galfarsoro, A. McCloskey, S. Zarate, X. Hernández and G. Almandoz, "Influence of manufacturing tolerances and eccentricities on the unbalanced magnetic pull in permanent magnet synchronous motors," 2020 International Conference on Electrical Machines (ICEM), 2020, pp. 1363-1369.

DOI: https://doi.org/10.1109/10.1109/ICEM49940.2020.9270843

© 2020 IEEE. Personal use of this material is permitted. Permission from IEEE must be obtained for all other uses, in any current or future media, including reprinting/republishing this material for advertising or promotional purposes, creating new collective works, for resale or redistribution to servers or lists, or reuse of any copyrighted component of this work in other works.

Influence of manufacturing tolerances and eccentricities on the unbalanced magnetic pull in permanent magnet synchronous motors

Unai Galfarsoro, Alex McCloskey, Sergio Zarate, Xabier Hernández, Gaizka Almandoz, Member, IEEE

***Abstract* – Eccentricity is an inevitable fault in electric motors and hence its diagnosis is an important topic. Thus, the influence of static and dynamic eccentricities on the harmonics of the frequency spectra of the unbalanced magnetic pull is analyzed.**

In this study, dimensional tolerances of the rotor and the stator are also considered. All parts have dimensional tolerances in their designs and their real magnitudes vary to some extent from the theoretical values after the manufacturing process. Thanks to the finite element simulations, verified with experimental results, it is observed that the deviations originated by the manufacturing tolerances produce changes in the amplitudes of some harmonics and also additional and characteristic harmonics in the frequency spectra of the unbalanced magnetic pull. These are not negligible and must be taken into account when robust eccentricity detection procedures are defined. Otherwise, harmonics originated by tolerances and by eccentricities can be misidentified.

***Index Terms* -- Fault detection, Fault diagnosis, Force measurement, Permanent magnet machines, Tolerance analysis.**

I. INTRODUCTION

The use of electric motors (EMs) is widespread, and is probably going to increase due to the ongoing success of electric vehicles. Yilmaz [1] states that the main kinds of EMs for plug-in hybrid electric vehicles are induction motors (IMs), permanent magnet synchronous motors (PMSMs), DC motors and switched reluctance motors. IMs and PMSMs are winning importance, and PMSMs are leaders in the market. Yilmaz [1] and Riba et al. [2] remark that PMSMs, compared to IMs, are less reliable and technologically mature.

Therefore, since PMSMs are a mass-produced product with a non-negligible danger of failure, it is justified to research the effect of their design on their reliability. According to Hong et al. [3], bearing faults, eccentricities and demagnetization of the permanent magnets (PMs) are the major causes of failures in PMSMs.

This paper analyzes the effect of static eccentricity (SE) and dynamic eccentricity (DE) by experimental measurements and by simulation. Eccentricity is a crucial defect that generates further magnetic and dynamic problems, torque ripple and unbalanced magnetic pull (UMP) [4], triggering additional vibrations and noise [5]. UMP is a radial force that remains fixed in space for SE and rotates with the rotor for DE [4][6]. Without eccentricity (WE) there would be no UMP. Hong et al. [3], Nandi et al. [7] and Ebrahimi et al. [8] declare that the lowest eccentricity value to take into account is about 5-10% of the air gap. Manufacturing and installation of the EMs create acceptable inherent eccentricity levels below 5-10%.

The experimental work is based on a modified version of the innovative test bench explained by Galfarsoro et al. in [9]. In this test bench SE is generated mounting the stator on a piezoelectric force sensor and supporting the rotor separately, as done by Chen et al. [6], Lee et al. [10] and Dorrell et al. [11]. The measurement of the UMP is possible with this decoupling of the stator and the rotor. These piezoelectric force sensors are costly, but their use is justified for research purposes. A second mechanism is incorporated into the test bench to create DE, by means of a rotor held by a shaft composed of two eccentric pieces that rotate between them [9].

Regarding simulations, the finite element (FE) method is used to calculate the UMP generated by eccentricities.

The originality of this study is that dimensional tolerances of the rotor and the stator are considered. All pieces have dimensional tolerances in their designs and their real magnitudes vary to some extend from the theoretical values after the manufacturing process. In the assembly process, in which all pieces of the EM are mounted together, the deviations of dimensions of all pieces are combined giving a final result that is not easy to predict unless a statistical tolerance analysis is carried out. This dimensional irregularities cause changes in the UMP of PMSMs, which may not be negligible compared to those that arise due to eccentricities, and thus have to be separated from the fault indicators to detect SE and DE.

Bramerdorfer [12] has carried out tolerance analysis for EM design optimization by statistical calculations, and observed as example the cogging torque and back-EMF sensitivity of an interior PMSM regarding changes in the material characteristics as well as a change in the PMs temperature. The results clearly indicate that the tolerance analysis is essential for the machine design.

Taran et al. [13] have studied three PM EMs with different configurations for dimensional and material tolerances, by FE simulation and by experimental measurements. A tolerance of ± 0.1 mm, considered typical for laser cutting prototyping, is considered for eleven

Orona EIC and the Basque Government (MECOVA ZL-2017/00457, MECOVA ZL-2018/00503 and MECOVA ZL-2019/00554) funded this research.

U. Galfarsoro, A. McCloskey, S. Zarate and G. Almandoz are with Mondragon Unibertsitatea, Mondragon, 20500, Spain (e-mail: ugalfarsoro@mondragon.edu, amccloskey@mondragon.edu, szarate@mondragon.edu, galmandoz@mondragon.edu).

X. Hernández is with Orona EIC, Hernani, 20120, Spain (e-mail: xhernandez@orona-group.com).

geometrical input design variables. Additionally, a ± 5% is considered for the PM remanence in order to account for possible variations both in the material grade and in the external magnetization. The effect of SE on the amplitude of the time signal of the back-EMF and cogging torque of an axial flux PM motor is analyzed. The conclusion is that variations in time signals are too small to have a sensitive enough method, and further studies based on frequency harmonics and side bands are suggested.

According to [13], a systematic study of dimensional and material tolerances is of the utmost importance in the process of designing and manufacturing an EM.

However, no papers that study the influence of eccentricity and manufacturing dimensional tolerances of the rotor and the stator on the UMP of PMSMs have been found.

Therefore, the first objective of this research is to study experimentally the influence of the manufacturing tolerances of the rotor and the stator on the spectra of the UMP with SE and DE. To achieve this objective, the real dimensions of the rotor and the stator are measured to assess their values. In addition, several SE and DE values are generated to measure the UMP of a PMSM accurately with the innovative experimental test bench. SE and DE coexist in real EMs, but are studied separately in this paper to simplify the analysis.

A second objective is to simulate by the FE method the previously measured cases.

The third objective is to compare experimental and simulation results, to obtain a good correlation, and as a result evaluate the independent influence of manufacturing tolerances and eccentricities on UMP. Beyond the calculation of UMP, this will help to have a reliable FE model to simulate the influence of manufacturing tolerances and eccentricities on other output variables like back-EMF, vibration, etc.

Finally, the last and most essential objective is to develop methods to diagnose the type (SE or/and DE) and severity of eccentricity faults in PMSMs with UMP, avoiding the disturbing influence of the manufacturing tolerances.

II. Analyzed Cases

In experimental measurements the PMSM under study has certain rotor and stator manufacturing dimensions that cannot be changed. Therefore, the study of manufacturing tolerances was carried out with only the initial values, and the changed variables were SE and DE.

In FE simulations the rotor and the stator were first simulated with the theoretical ideal dimensions, varying SE and DE. Then the experimentally measured real dimensions were implemented independently into the rotor, the stator, and both rotor and stator, varying SE and DE in each case.

III. Experimental Measurements of Dimensions

A. Measurement of the remanent magnetic field of magnets

Before mounting the PMs on the rotor, they were magnetized carefully and their magnetization levels were measured using a magnetic characterizer one by one to minimize the effect of their dispersion. The biggest deviation of the magnetization level of one magnet from the mean magnetization level was only 0.26%.

B. Measurement of critical dimensions

The theoretical diameters of the teeth of the stator and the poles of the rotor are known from their drawings. However, dimensions of parts vary according to manufacturing tolerances. Thus, both diameters were measured on the manufactured PMSM and these real dimensions were used later when the geometry of the FE model was built.

1) Measurement of the Qs = 36 teeth of the stator:

The stator was positioned on the table of a three-dimensional coordinate measuring machine (CMM) and its inner cylindrical bore formed by the teeth was measured (Fig. 1). The diameter of each one of the *Qs* = 36 teeth was measured in 16 points by a contact probe, having a total of 36 x 16 = 576 measured points. Next, the mean of the 16 values was calculated for each tooth and taken as the nominal value of the diameter of the tooth (see these results in Table I). The relative error of Table I was calculated relative to the air gap of 1 mm. Results suggested that deviations of the real diameters of the teeth from the theoretical diameters exceeded values of 5% in most cases and even values of 11% for some teeth. Taking into account that values of eccentricity in the range of 5-10% are considered as residual [3][7][8], the measured values were close or even out of the upper suggested limit.

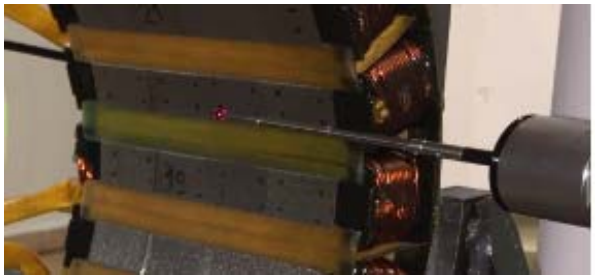

Fig. 1. Measurement of the teeth of the stator in a three-dimensional coordinate measuring machine

TABLE I
TRUE VALUES OF THE DIAMETERS OF THE TEETH OF THE STATOR, MEASURED IN A THREE-DIMENSIONAL COORDINATE MEASURING MACHINE: CALCULATIONS BASED ON MEAN VALUES FOR EACH TOOTH (ONLY VALUES OF 1 OUT OF 3 TEETH ARE SHOWN FOR CONCISENESS)

Tooth number	Mean diameter (mm)	Absolute error (mm)	Relative error (%)	
1	221,956	-0,044	-4,41%	
4	222,053	0,053	5,29%	
7	222,093	0,093	9,25%	
10	221,890	-0,110	-10,99%	Minimum diameter
13	222,063	0,063	6,27%	
16	222,114	0,114	11,45%	Maximum diameter
19	221,917	-0,083	-8,32%	
22	222,080	0,080	8,02%	
25	222,104	0,104	10,42%	
28	221,890	-0,110	-10,98%	
31	222,046	0,046	4,55%	
34	222,104	0,104	10,44%	

Nevertheless, if calculations were based on individual points measured in all teeth, deviations from theoretical diameter values were even bigger, as shown in Table II.

TABLE II
TRUE VALUES OF THE DIAMETERS OF THE TEETH OF THE STATOR, MEASURED IN A THREE-DIMENSIONAL COORDINATE MEASURING MACHINE. CALCULATIONS BASED ON MEAN VALUES FOR EACH TOOTH VS. CALCULATIONS BASED ON INDIVIDUAL POINTS MEASURED IN ALL TEETH

Calculations based on mean values for each tooth		Calculations based on individual points measured in all teeth	
Maximum diameter (mm)	Minimum diameter (mm)	Maximum diameter (mm)	Minimum diameter (mm)
222,114	221,890	222,269	221,819
Absolute error (mm)	Absolute error (mm)	Absolute error (mm)	Absolute error (mm)
0,114	-0,110	0,269	-0,181
Relative error (%)	Relative error (%)	Relative error (%)	Relative error (%)
11,45%	-10,99%	26,92%	-18,09%
Absolute peak-peak error (mm)		Absolute peak-peak error (mm)	
0,224		0,450	
Relative error (%)		Relative error (%)	
22,44%		45,01%	

2) Measurement of the p = 15 pole pairs of the rotor:

The rotor was positioned on its shaft in the PMSM and its outer cylinder was measured using a dial indicator (Fig. 2). Each of the $2p = 30$ poles was measured in 16 points, having a total of 30 x 16 = 480 measured points. Next, the mean of the 16 values was calculated and taken as the nominal deviation of the pole from the theoretical diameter value (see these results in Table III). Results suggest that deviations of the real diameters of the poles from the theoretical diameters were small, much smaller than for the bore of the stator, and inside the range of 5-10% mentioned beforehand as residual for eccentricity [3][7][8]. In spite of their small value, they were taken into account in the FE model.

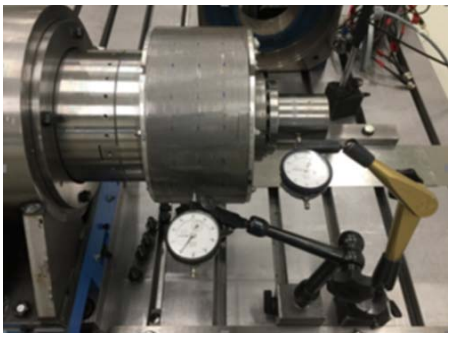

Fig. 2. Measurement of the poles of the rotor by means of dial indicators

TABLE III
TRUE VALUES OF THE DIAMETERS OF THE POLES OF THE ROTOR, MEASURED WITH DIAL INDICATORS: CALCULATIONS BASED ON MEAN VALUES FOR EACH POLE (ONLY VALUES OF 1 OUT OF 3 POLES ARE SHOWN FOR CONCISENESS)

Pole number	Absolute error (mm)	Relative error (%)	
1	0,0087	0,87%	
4	-0,0061	-0,61%	
7	-0,0114	-1,14%	
10	-0,0131	-1,31%	
13	0,0036	0,36%	
16	0,0131	1,31%	
19	-0,0058	-0,58%	
22	-0,0304	-3,04%	Minimum diameter
25	-0,0042	-0,42%	
28	0,0217	2,17%	Maximum diameter

IV. EXPERIMENTAL TEST BENCH

The experimental test bench is based on the concept explained by Galfarsoro et al. [9]. In that study a PMSM with a decoupled rotor and stator was designed and built, enabling the generation of any value of SE and/or DE in a continuous and controlled way. The test bench was equipped with a force transducer located under the stator to measure the UMP and search coils located on the teeth to measure the back-EMF and consequently the magnetic field in the air gap. Results obtained from the measurement of both variables showed that the test bench was suitable to generate SE and/or DE, and to be used to measure different variables to diagnose faults in EMs. Other sensors like accelerometers and a position-measuring laser were also used for additional future work.

In the present study the abovementioned test bench is connected to a second EM (Fig. 3). The second EM drives the PMSM under test so that it works in open circuit. The objective is to avoid the influence of the control on the PMSM under test, since the control can inject harmonics in the current that are later seen in other measured variables, modifying the effect of the defects (tolerances and eccentricities) analyzed.

Regarding control, the second EM is fed by an inverter, which controls the chosen constant speed. The speed controller is tuned so as to have low speed ripple.

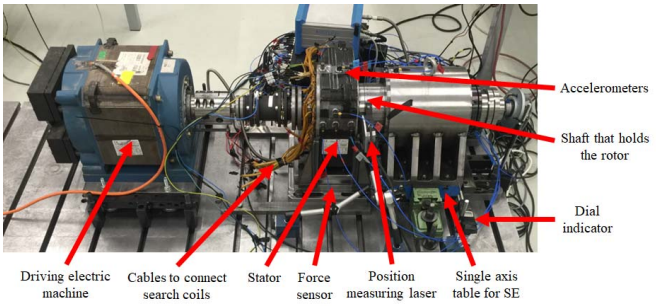

Fig. 3. Experimental test bench for the measurements of the UMP

V. ELECTROMAGNETIC FE SIMULATIONS

A. Analyzed cases

Three eccentricity cases were considered in the FE simulations: without eccentricity, with static eccentricity and with dynamic eccentricity. Within each of these three cases, four kinds of tolerances were simulated: 1) Without tolerance (both rotor and stator with the theoretical dimensions, that is, the ideal case); 2) With only rotor tolerances; 3) With only stator tolerances; 4) With both rotor and stator tolerances.

B. Description of the electromagnetic FE simulations

As explained before, the EM has manufacturing tolerances that cannot be disregarded. Referring to the diameters of the poles of the rotor, in order to create the geometry easier, all the poles had the same diameter and the magnet associated to each pole had a correction factor to take into account the different air gap of each pole. Therefore, each magnet had its particular remanence according to the diameter of its pole. The stator teeth had the experimentally measured real dimensions, hence not all the teeth were equal. The eccentricity grade modeled was 55% of the air gap. For each simulation the magnitude of the UMP was calculated.

VI. RESULTS FOR STATIC ECCENTRICITY

A. Results of the experimental measurements

The Fast Fourier Transforms (FFTs) of the measured UMPs for increasing values of SE are shown in Fig. 4 (note: all FFTs in this paper are with the abscissa in harmonics of the fundamental electric order). These results confirm that SE changes the frequency content of the UMP, increasing some characteristic orders and decreasing others. Fig. 5 is a zoom of Fig. 4 to highlight two representative electric orders.

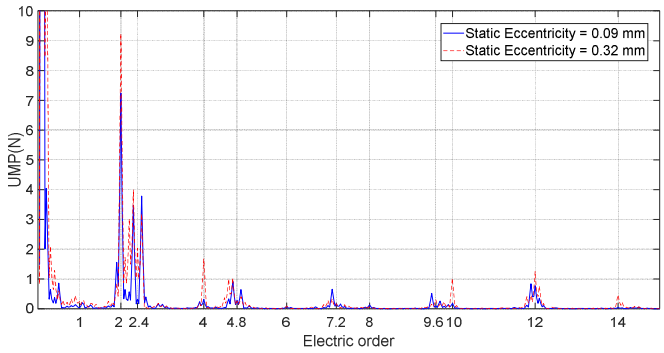

Fig. 4. FFT of the experimental UMP for an increasing value of static eccentricity

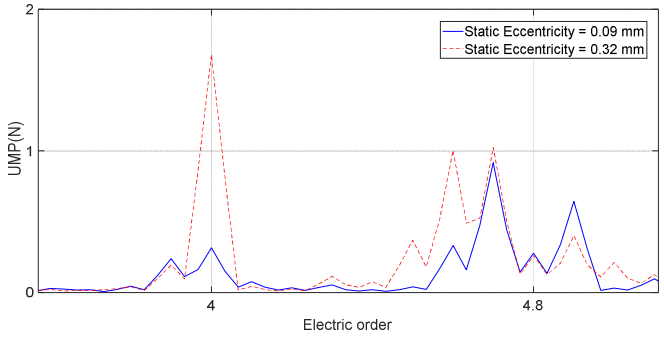

Fig. 5. FFT of the experimental UMP for an increasing value of static eccentricity. Zoom of electric orders 4 and 4.8

B. Results of the electromagnetic FE simulations

Fig. 6 shows the simulated spectra of the UMP, with both rotor and stator real dimensions. Blue peaks of electric orders correspond to the spectrum WE, and red peaks of electric orders to the spectrum with 55% SE. The conclusion is that generally electric orders 2, 4, 6, etc. (multiples of 2) increase without sideband peaks, whilst electric orders 2.4, 4.8, 7.2, etc. (multiples of Qs/p) decrease and their sideband peaks, which are separated $1/p$, increase. Fig. 7 displays two of these electric orders in detail to observe the abovementioned effect.

Fig. 6 takes into account the simultaneous effect of rotor and stator tolerances in the UMP with SE. Alternatively, Fig. 8 and Fig. 9 break down and separate the effect of each of the tolerances on SE. Red peaks of electric orders in Fig. 8 confirm that, if tolerances are disregarded, a SE only generates peaks that are multiples of 2. Comparing green peaks vs. red peaks in Fig. 9, the conclusion is that rotor tolerances generate the increase of electric orders 2.4, 4.8, 7.2, etc. (multiples of Qs/p) and the increase of their sideband peaks that are separated $1/p$. Comparing orange peaks vs. red peaks in Fig. 9, the conclusion is that stator tolerances generate the increase of electric orders 2, 4, 6, etc. (multiples of 2) without sideband peaks.

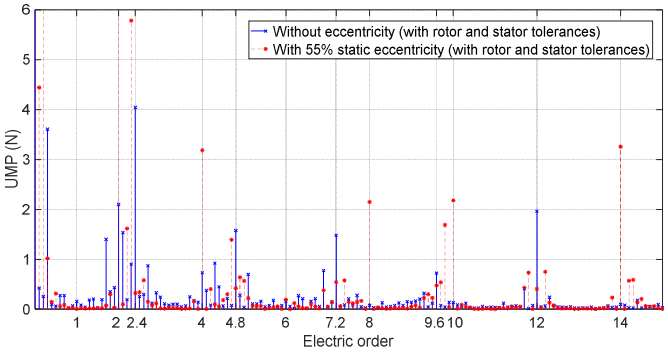

Fig. 6. FFT of the simulated UMP for an increasing value of static eccentricity. Rotor and stator with tolerances

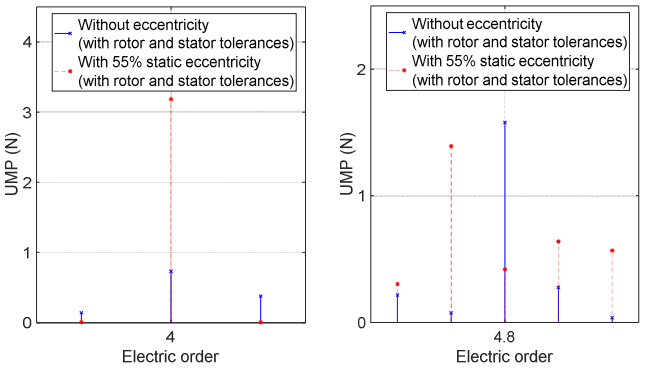

Fig. 7. FFT of the simulated UMP for an increasing value of static eccentricity. Rotor and stator with tolerances. Zoom of electric orders 4 (left) and 4.8 (right)

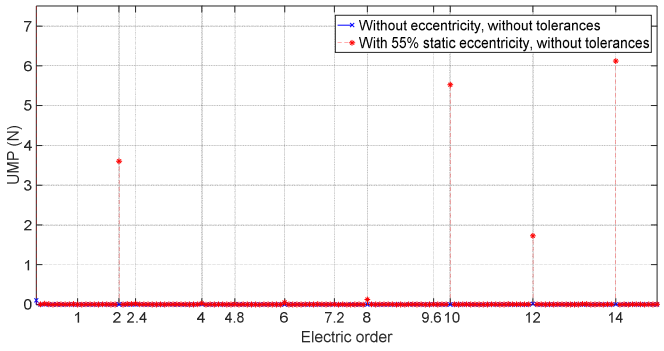

Fig. 8. Effect of static eccentricity on the FFT of the simulated UMP, without tolerances

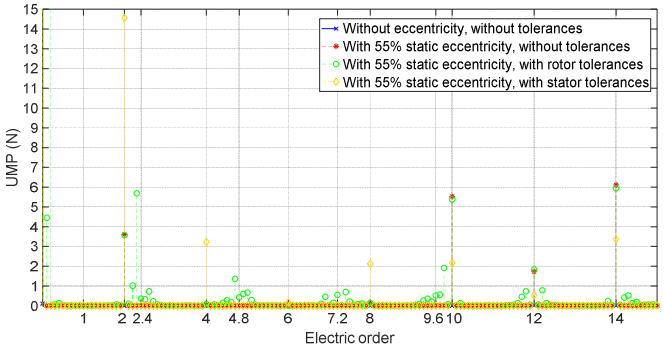

Fig. 9. Effect of tolerances on the FFT of the simulated UMP, with static eccentricity

C. *Correlation between experimental and simulation results*

Experimental results are only measurable with real manufacturing dimensions on the PMSM under test. Hence, only the cases with both rotor and stator tolerances are going to be compared next.

Regarding SE results, comparison of Fig. 4 for experimental results and Fig. 6 for simulation results produces similar general tendencies in the UMP. That is, a SE generates the increase of electric orders 2, 4, 6, etc. (multiples of 2) without sideband peaks, and variations on the amplitudes of electric orders 2.4, 4.8, 7.2, etc. (multiples of Qs/p) and especially their sideband peaks that are separated $1/p$.

VII. RESULTS FOR DYNAMIC ECCENTRICITY

A. *Results of the experimental measurements*

The FFTs of the measured UMPs for increasing values of DE are shown in Fig. 10. These results confirm that DE also changes the frequency content of the UMP, increasing some characteristic orders and decreasing others. Fig. 11 is a zoom of Fig. 10 to highlight two representative electric orders.

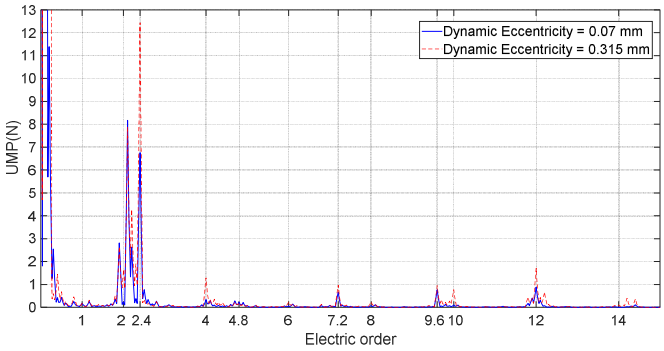

Fig. 10. FFT of the experimental UMP for an increasing value of dynamic eccentricity

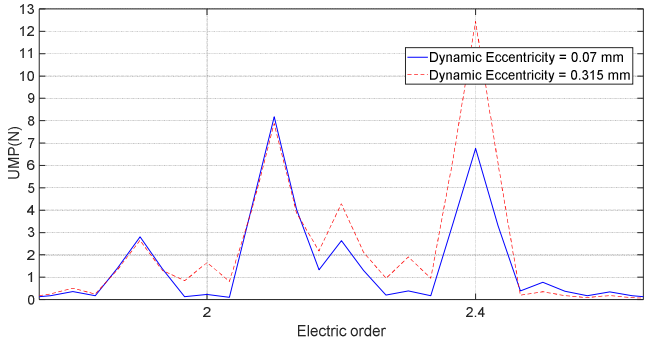

Fig. 11. FFT of the experimental UMP for an increasing value of dynamic eccentricity. Zoom of electric orders 2 and 2.4

B. *Results of the electromagnetic FE simulations*

Fig. 12 shows the simulated spectra of the UMP with both rotor and stator real dimensions. Blue peaks of electric orders correspond to the spectrum WE, and red peaks of electric orders to the spectrum with 55% DE. The conclusion is that generally electric orders 2, 4, 6, etc. (multiples of 2) increase and their sideband peaks that are separated $1/p$ also increase, whilst electric orders 2.4, 4.8, 7.2, etc. (multiples of Qs/p) increase without sideband peaks. Fig. 13 displays two of these electric orders in detail to observe the abovementioned effect.

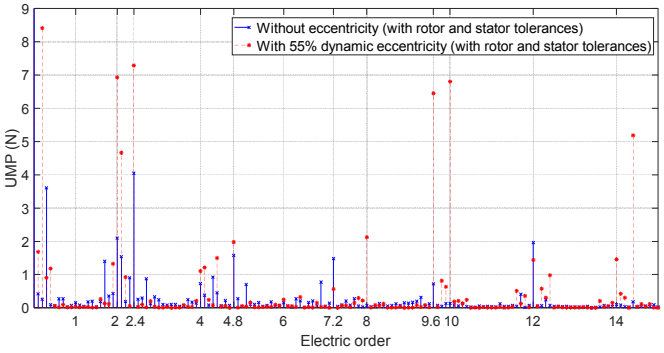

Fig. 12. FFT of the simulated UMP for an increasing value of dynamic eccentricity. Rotor and stator with tolerances

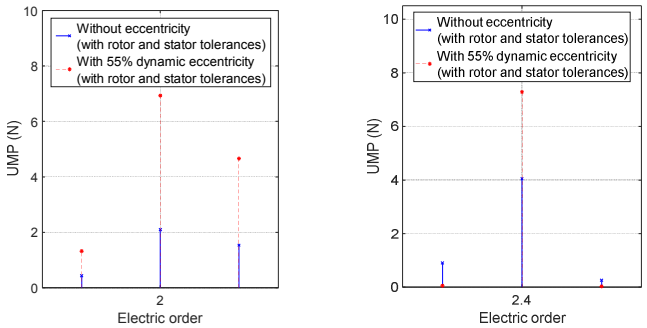

Fig. 13. FFT of the simulated UMP for an increasing value of dynamic eccentricity. Rotor and stator with tolerances. Zoom of electric orders 2 (left) and 2.4 (right)

Fig. 12 takes into account the simultaneous effect of rotor and stator tolerances in the UMP with DE. Alternatively, Fig. 14 and Fig. 15 break down and separate the effect of each of the tolerances on DE. Red peaks of electric orders in Fig. 14 confirm that, if tolerances are disregarded, a DE only generates peaks that are multiples of Qs/p. Comparing green peaks vs. red peaks in Fig. 15, the conclusion is that rotor tolerances generate the increase of electric orders 2.4, 4.8, 7.2, etc. (multiples of Qs/p) without sideband peaks. Comparing orange peaks vs. red peaks in Fig. 15, the conclusion is that stator tolerances generate the increase of electric orders 2, 4, 6, etc. (multiples of 2) and of their sideband peaks that are separated $1/p$.

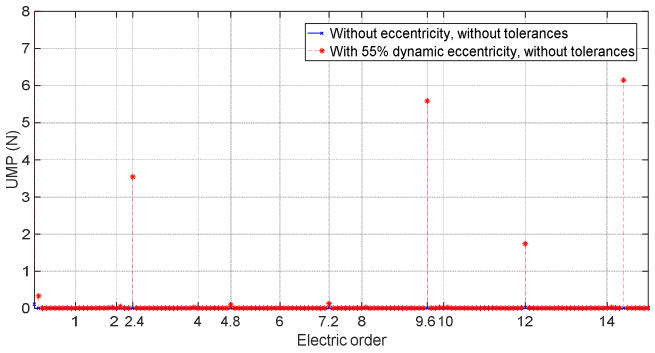

Fig. 14. Effect of dynamic eccentricity on the FFT of the simulated UMP, without tolerances

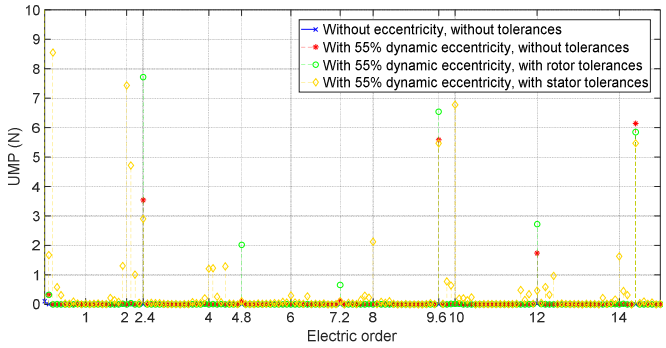

Fig. 15. Effect of tolerances on the FFT of the simulated UMP, with dynamic eccentricity

This paper bases the analysis on the magnitude of the UMP. Nevertheless, some works take into account the projection of the UMP on a fixed direction. In that case, results are different for both SE and DE, and a comment is necessary. As an example, Fig. 16 shows the UMP in the fixed horizontal X direction simulated for DE. This figure is the analogous to Fig. 12 but for the UMP in a fixed direction. The interesting remark is that in Fig. 12 electric orders multiples of 2, their 1/*p* separated sideband peaks and electric orders multiples of *Qs*/*p* are prominent, whilst in Fig. 16 generally electric orders multiples of 2 and *Qs*/*p* are smaller, 1/*p* separated sideband peaks of multiples of 2 are bigger and multiples of *Qs*/*p* have new 1/*p* separated sideband peaks. Besides, the biggest electric order for the UMP in the fixed X direction is 1/*p*, instead of order 0 as it occurs for all previous spectra obtained for the magnitudes of the UMP.

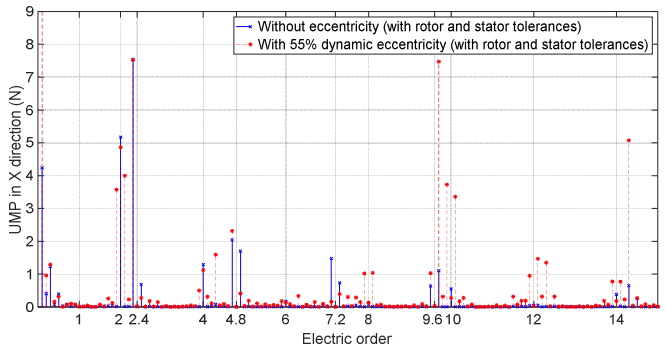

Fig. 16. FFT of the simulated UMP in fixed horizontal X direction for an increasing value of dynamic eccentricity. Rotor and stator with tolerances

C. *Correlation between experimental and simulation results*

Analyzing DE results, Fig. 10 and Fig. 12 for experimental and simulation results respectively also give similar overall trends in the UMP. Namely, a DE generates the increase of electric orders 2, 4, 6, etc. (multiples of 2) with sideband peaks that are separated 1/*p*, and the increase of electric orders 2.4, 4.8, 7.2, etc. (multiples of *Qs*/*p*) without sideband peaks.

VIII. Summary of FE Simulation Results

The main orders in the simulation FFTs are summarized in Table IV for the PMSM WE, with SE and with DE. These orders are shown as mechanical orders for simplicity (divide all values by *p* to obtain electric orders). The conclusion from these FE simulations is that SE and DE generate new peaks in the spectra of UMP, and that these peaks are dependent on the dimensional tolerances of the rotor and the stator diameters.

TABLE IV
MAIN MECHANICAL ORDERS IN THE UMP WITHOUT ECCENTRICITY, WITH STATIC ECCENTRICITY AND WITH DYNAMIC ECCENTRICITY, DEPENDING ON TOLERANCE TYPE

Without eccentricity			
Ideal	**Rotor tolerance**	**Stator tolerance**	**Rotor + Stator tolerance**
	○ 0 [1)] ○ *Qs* * *k*	○ 0 [1)] ○ 2*p* * *k*	○ 0 [1)] ○ *Qs* * *k* ○ 2*p* * *k*
With static eccentricity			
Ideal	**Rotor tolerance**	**Stator tolerance**	**Rotor + Stator tolerance**
0 [2)] LCM(*Qs*, 2*p*) * *k* LCM(*Qs*, 2*p*) * *k*± 2*p* * *m*	0 [2)] LCM(*Qs* ,2*p*) * *k* LCM(*Qs* ,2*p*) * *k* ±2*p* * *m* 1 [1)] *Qs* * *k* *Qs* * *k* ±1,2,3...	0 [2)] LCM(*Qs* ,2*p*) * *k* LCM(*Qs* ,2*p*) * *k* ±2*p* * *m* 2*p* * *k*	0 [2)] LCM(*Qs* ,2*p*) * *k* LCM(*Qs* ,2*p*) * *k* ±2*p* * *m* 1 [1)] *Qs* * *k* *Qs* * *k* ±1,2,3… 2*p* * *k*
With dynamic eccentricity			
Ideal	**Rotor tolerance**	**Stator tolerance**	**Rotor + Stator tolerance**
0 [2)] LCM(*Qs*, 2*p*) * *k* LCM(*Qs*, 2*p*) * *k*±*Qs* * *m*	0 [2)] LCM(*Qs*, 2*p*) * *k* LCM(*Qs*, 2*p*) * *k*±*Qs* * *m* *Qs* * *k*	0 [2)] LCM(*Qs* ,2*p*) * *k* LCM(*Qs* ,2*p*) * *k* ±*Qs* * *m* 1 [1)] 2*p* * *k* 2*p* * *k* ±1,2,3...	0 [2)] LCM(*Qs* ,2*p*) * *k* LCM(*Qs* ,2*p*) * *k* ±*Qs* * *m* *Qs* * *k* 1 [1)] 2*p* * *k* 2*p* * *k* ±1,2,3...

[1)]: Biggest amplitude in FFT, with values around 5 to 10 N
[2)]: Biggest amplitude in FFT, with values around 2145 N
k = 0, 1, 2, 3… m = 0, 1, 2, 3… LCM: Least Common Multiple

IX. Conclusions

The UMP of a PMSM was measured experimentally and calculated by FE simulation with similar trends in results. The main conclusion is that the frequency components of the UMP with eccentricity depend not only on the type and level of eccentricity, but also on the tolerances of the diameters of the rotor and the stator (and presumably on the tolerances of other dimensions of the parts of the motor and the magnetization levels of the magnets). Furthermore, the influence of the tolerances is significant, since some of the biggest peaks in the FFT of the UMP only exist if the tolerances are present. The amplitudes of those harmonics are subjected to the manufacturing tolerances, so they change from one motor unit to another. Therefore, a robust eccentricity detection procedure must consider this. Otherwise, erroneous eccentricity estimations can be given and harmonics originated by tolerances and by eccentricities can be misidentified.

To sum up, the electric orders that arise in UMP with SE without the influence of tolerances are the same that change with stator tolerances (multiples of 2). With DE the electric orders generated are those that appear with rotor tolerances (multiples of *Qs*/*p*). Therefore, the amplitudes of these harmonics are subjected to eccentricity and tolerances. However, some differences were observed that may help to obtain a reliable eccentricity detection procedure. With tolerances, for SE, multiples of *Qs*/*p* have side bands that can be good indicators. Similarly, for DE the side bands of the multiples of 2 are the ones to take into account. Nevertheless,

the amplitudes are subjected to tolerances, and thus, a deeper analysis considering more eccentricity and tolerance levels is needed.

X. APPENDIX

TABLE 5
PMSM UNDER TEST MAIN SPECIFICATIONS

Pole pairs (p)	15
Number of slots of the stator (Qs)	36
Rotor outer diameter / length	220 mm / 100 mm
Stator inner diameter / length	222 mm / 100 mm
Air gap	1 mm
Rated speed	96 rpm

XI. ACKNOWLEDGMENT

The authors gratefully acknowledge the contributions of B. Arregi, J.M. Iriondo, J. Fuente, J. Grande, T. Antunez, A. Villar, J. Maskariano, G. Arrizabalaga, L. Azpitarte, G. Aretxaga, J. Larrañaga, I. Ezpeleta, A. Arana, I. Eraña, and others, for their work on the design, manufacturing, assembly and final tuning of the test bench.

XII. REFERENCES

[1] M. Yilmaz, "Limitations/capabilities of electric machine technologies and modeling approaches for electric motor design and analysis in plug-in electric vehicle applications," *Renewable and Sustainable Energy Reviews*, vol. 52, pp. 80–99, 2015.

[2] J. R. Riba, C. López-Torres, L. Romeral, and A. Garcia, "Rare-earth-free propulsion motors for electric vehicles: A technology review," *Renewable and Sustainable Energy Reviews*, vol. 57, pp. 367–379, May 2016.

[3] J. Hong, S. Park, D. Hyun, T. Kang, S. B. Lee, C. Kral, and A. Haumer, "Detection and classification of rotor demagnetization and eccentricity faults for PM synchronous motors," *IEEE Transactions on Industry Applications*, vol. 48, no. 3, pp. 923–932, May 2012.

[4] *VDI 3839-5:2001. Instructions on measuring and interpreting the vibration of machines - Typical vibration patterns with electrical machines*. VDI (The Association of German Engineers), 2001.

[5] W. le Roux, R. G. Harley, and T. G. Habetler, "Detecting Rotor Faults in Low Power Permanent Magnet Synchronous Machines," *IEEE Transactions on Power Electronics*, vol. 22, pp. 322–328, Jan. 2007.

[6] X. Chen, Z. Deng, J. Hu, and T. Deng, "An analytical model of unbalanced magnetic pull for PMSM used in electric vehicle: Numerical and experimental validation," *International Journal of Applied Electromagnetics and Mechanics*, vol. 54, no. 4, pp. 583–596, 2017.

[7] S. Nandi, H. A. Toliyat, and X. Li, "Condition Monitoring and Fault Diagnosis of Electrical Motors - A Review," *IEEE Transactions on Energy Conversion*, vol. 20, pp. 719–729, Dec. 2005.

[8] B. M. Ebrahimi, M. J. Roshtkhari, J. Faiz, and S. V. Khatami, "Advanced eccentricity fault recognition in permanent magnet synchronous motors using stator current signature analysis," *IEEE Transactions on Industrial Electronics*, vol. 61, no. 4, pp. 2041–2052, Apr. 2014.

[9] U. Galfarsoro, A. McCloskey, X. Hernandez, G. Almandoz, S. Zarate, and X. Arrasate, "Eccentricity detection procedure in electric motors by force transducer and search coils in a novel experimental test bench," in *2019 IEEE 12th International Symposium on Diagnostics for Electrical Machines, Power Electronics and Drives (SDEMPED)*, 2019, pp. 220–226.

[10] C. I. Lee and G.-H. Jang, "Experimental measurement and simulated verification of the unbalanced magnetic force in brushless DC motors," *IEEE Transactions on Magnetics*, vol. 44, no. 11, pp. 4377–4380, 2008.

[11] D. Dorrell and A. Smith, "Calculation and measurement of unbalanced magnetic pull in cage induction motors with eccentric rotors. II. Experimental investigation," *IEE Proceedings-Electric Power Applications*, vol. 143, no. 3, pp. 202–210, 1996.

[12] G. Bramerdorfer, "Tolerance Analysis for Electric Machine Design Optimization: Classification, Modeling and Evaluation, and Example," *IEEE Transactions on Magnetics*, vol. 55, no. 8, pp. 1–9, 2019.

[13] N. Taran, V. Rallabandi, D. M. Ionel, P. Zhou, M. Thiele, and G. Heins, "A systematic study on the effects of dimensional and materials tolerances on permanent magnet synchronous machines based on the IEEE Std 1812," *IEEE Transactions on Industry Applications*, vol. 55, no. 2, pp. 1360–1371, 2018.

XIII. BIOGRAPHIES

Unai Galfarsoro was born in Saint-Jean-de-Luz, France. He received the B.Sc. and M.Sc. degrees in Mechanical Engineering and Industrial Engineering from Mondragon Unibertsitatea in 1991 and 2004 respectively. In 1993 he received the M.Phil. degree from the University of Northumbria at Newcastle.

Since 1993, he has been with the Acoustics and Vibrations Group of the Mechanics and Manufacturing department of the Faculty of Engineering of Mondragon Unibertsitatea, where he is currently a Lecturer and Researcher. His current research interests include noise source identification, and electrical machines diagnosis. He has participated in a number of research projects in the fields of elevator drives, household appliances, machine tools, etc.

Alex McCloskey was born in Dublin, Ireland. He received the B.Sc. and M.Sc. degrees in Mechanical Engineering and Industrial Engineering from Mondragon Unibertsitatea in 2009 and 2012 respectively. He developed his Ph.D. thesis about vibrations of electrical machines in Mondragon Unibertsitatea.

Since 2016, he has been with the Acoustics and Vibrations Group of the Mechanics and Manufacturing department of the Faculty of Engineering of Mondragon Unibertsitatea, where he is currently a Lecturer and Researcher. His current research interests include electrical machines design and diagnosis. He has participated in a number of research projects in the fields of elevator drives and railway traction.

Sergio Zarate was born in Vitoria-Gasteiz, Spain. He received the B.Sc., M.Sc. and Ph.D. degrees in electrical engineering at Mondragon Unibertsitatea, Mondragon, Spain, in 2012, 2014 and 2018, respectively.
Since 2018, he has been with the Electronics department of the Faculty of Engineering of Mondragon Unibertsitatea, where he is currently a Lecturer and Researcher. His current research interests include drives, electrical machines vibration and permanent magnet machine design and optimization.

Xabier Hernández was born in Pasaia, Spain. He received the B.Sc. and M.Sc. degrees in Mechanical Engineering and Industrial Engineering from Mondragon Unibertsitatea in 2008 and 2011 respectively.

Since 2011, he works in Orona S. Coop. where he currently is in charge of the Vibroacoustics research team. During this period, he has participated in several industrial research projects. His current research interests include electrical machines design, vibroacoustic design and diagnosis.

Gaizka Almandoz was born in Arantza, Spain. He received the B.Sc. and Ph.D. degrees in electrical engineering at Mondragon Unibertsitatea, Mondragon, Spain, in 2003 and 2008, respectively.

Since 2003, he has been with the Electronics, Faculty of Engineering, Mondragon Unibertsitatea, where he is currently an Associate Professor. His current research interests include electrical machine design, modelling and control. He has participated in various research projects in the fields of wind energy systems, elevator drive and railway traction.